

LYAPUNOV GUIDANCE: STABILIZING GENERATIVE FLOWS WITH ONE-LINE CODE

Anonymous authors

Paper under double-blind review

ABSTRACT

Flow matching has recently emerged as a powerful approach to learning complex data distributions with excellent performance across diverse generative tasks, yet adapting pre-trained flow models to new tasks typically requires costly retraining. To mitigate this issue, post-training guidance methods were proposed as they are lightweight and user-friendly for downstream applications. However, existing guidance methods are unreliable since they usually rely on function approximations and lack structural guarantees of sampling stability. In this paper, we address this challenge by proposing a unified framework, LyaGuide (Lyapunov Guidance for flow matching), which reformulates the guidance in flow matching as a Lyapunov control problem. LyaGuide supports two modes depending on whether the Lyapunov function is a known priori: a model-driven mode for developer-oriented scenarios where the guidance distribution is explicitly specified, and a data-driven mode for user-oriented scenarios where pre-trained models can be adapted with downstream task-specific data. Furthermore, to enforce the stability, we introduce a pseudo projection operator with a closed-form expression that strictly satisfies the Lyapunov condition. Notably, LyaGuide is compatible with any guidance method and can be implemented with a single line of code. Experiments on synthetic datasets and image inverse problems demonstrate that our framework consistently improves sample quality and guidance fidelity while preserving efficiency, and it significantly enhances the performance of existing guidance methods.

1 INTRODUCTION

Generative modeling has recently witnessed remarkable progress with the advent of diffusion models (Song et al., 2021; Dhariwal & Nichol, 2021; Ho & Salimans) as well as their deterministic counterparts based on flow matching (Lipman et al., 2023; Liu et al., 2023b; Tong et al., 2023). Flow matching learns a time-dependent vector field that transfers an easy-to-sample base distribution to a complex data distribution, providing a mathematically elegant and computationally efficient alternative compared to stochastic diffusion processes. Nevertheless, it is still hard to adapt a pre-trained flow model to achieve fantastic performance in downstream applications by retraining with corresponding task-specific data, which is straightforward but suffers from a heavy and inflexible workflow. In contrast, post-training guidance methods are more lightweight and efficient for adaption, while existing approaches are almost heuristic or approximation based Fan et al. (2025); Feng et al. (2025), lacking theoretical guarantees on the stability of the guided generation process. This urgently calls for a unified theoretical framework that unifies diverse conditions, including class labels (Dhariwal & Nichol, 2021; Ho & Salimans), structural constraints in molecular design (Zhang et al., 2024b), and reward functions in reinforcement learning (Jan-

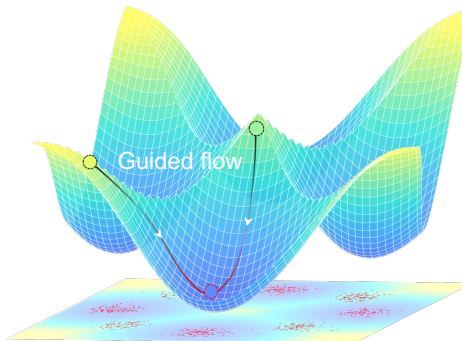


Figure 1: Lyapunov landscape for 8-Gaussian guidance from initial (black dashed) to target data (red dashed), defined as the negative of the energy landscape.

ner et al., 2022), while providing both improved performance and rigorous stability guarantees for guided flows.

An analogous challenge has long been studied in cybernetics, where the central objective is to steer the dynamics to the target states. Previous works employ Lyapunov stability theory to design stabilizing policies for linear or polynomial systems, such as the linear quadratic regulator (LQR) (Khalil, 2002) and the semidefinite programming (SDP) based sum-of-squares (SOS) methods (Parrilo, 2000). For more intricate high-dimensional and nonlinear dynamics, recent work has integrated machine learning into control (Tsukamoto et al., 2021). In particular, neural controllers are trained jointly with certificate functions, such as Lyapunov functions, LaSalle’s invariants, barrier certificates, and contraction metrics (Chang et al., 2019; Zhang et al., 2022a; Yang et al., 2025; Zhang et al., 2022b; Qin et al., 2020; Sun et al., 2021).

In this work, we propose a unified flow matching guidance framework from the perspective of *Lyapunov control theory* (Artstein, 1983; Sontag, 1989; Polyakov, 2012), where the energy function that determines the conditional distribution is interpreted as a Lyapunov function, while the added guidance term serves as a stabilizing control input. This equivalence allows us to reinterpret a wide range of existing guidance strategies as special cases of Lyapunov control, as shown in Fig. 1, including classifier guidance, classifier-free guidance, energy-based guidance, and reward-guided generation. In addition to providing theoretical clarity, we also introduce *pseudo projection operation* that enforces the Lyapunov condition on the guidance, ensuring that the guided flows could converge to the target distribution (see Section 4). Thus, our approach unifies diverse guidance strategies within a Lyapunov framework, providing both theoretical guarantees and practical efficiency.

Although the control-theoretic view offers strong guarantees, a practical challenge is how to obtain the Lyapunov function V that encodes prior knowledge. Sometimes V can be written explicitly (for example, classifier guidance with $V(\mathbf{x}) = -\log p(y|\mathbf{x})$ in image generation (Dhariwal & Nichol, 2021) or structural energy terms in protein design (Zhang et al., 2024b)), while in many other applications prior knowledge is only implicitly available through few-shot supervised learning Janner et al. (2022); Lee et al. (2025); Black et al. (2023). To address this, we propose to *learn Lyapunov functions from limited data of downstream tasks*, and then design guidance policies based on the learned Lyapunov function.

Contribution. The principal contributions of this work can be summarized as follows:

- We establish a unified theoretical framework that unifies diverse guidance strategies in flow matching as instances of Lyapunov control, thereby providing a common foundation for guided generative modeling.
- We propose a pseudo projection operator with a closed-form expression that enforces Lyapunov stability for any candidate guidance function, achieving rigorous guidance with a single-line code implementation.
- Building on our theory, we introduce **LyaGuide**, which is adaptive to different scenarios and offers several efficient variants. These variants enable users to trade off between flexibility and strictness of stability guarantees depending on the downstream task.
- We validate the proposed framework on synthetic datasets and image inverse problems, where it significantly improves the sample quality of baselines while preserving computational efficiency. The code for reproducing the results is available at `anonymous/LyaGuide`.

Due to the limit of page, we summarise the **Related Work** in Appendix A.3.

2 BACKGROUND

2.1 FLOW MATCHING

Flow matching (Lipman et al., 2023) is a ODE-based training framework for generative modeling, which learns continuous-time dynamics that transforms a simple prior distribution to a complex data distribution. Formally, let p_0 and p_1 denote the source and target distributions over \mathbb{R}^d , respectively. flow matching aims to learn a time-dependent vector field $\mathbf{u}(\mathbf{x}, t) \triangleq \mathbf{u}_t(\mathbf{x}) : \mathbb{R}^d \times [0, 1] \rightarrow \mathbb{R}^d$ that pushes p_0 to p_1 along a continuous path $\{p_t\}_{t \in [0, 1]}$, such that the flow ϕ_t governed by the ODE:

$$\frac{d\phi_t(\mathbf{x})}{dt} = \mathbf{u}_t(\phi_t(\mathbf{x})), \quad \phi_0(\mathbf{x}) = \mathbf{x}, \quad (1)$$

transfers $\mathbf{x} \sim p_0$ to a sample $\phi_1(\mathbf{x}) \sim p_1$.

To learn a neural field $\hat{\mathbf{u}}_\theta(\mathbf{x}, t)$ that matches the continuous path $\{p_t\}_{t \in [0,1]}$, a convenient way to define targets is via a latent variable $z \sim p(z)$ that indexes conditional bridges $p_t(\mathbf{x}_t | z)$ together with conditional vector fields $\mathbf{u}_{t|z}(\mathbf{x}_t | z)$. This induces the marginal path and vector field $p_t(\mathbf{x}_t) = \int p_t(\mathbf{x}_t | z) p(z) dz$, $\mathbf{u}_t(\mathbf{x}_t) = \int \mathbf{u}_{t|z}(\mathbf{x}_t | z) p(z | \mathbf{x}_t) dz$, and it is known that \mathbf{u}_t generates the marginal path p_t (see (Lipman et al., 2023)). To avoid the intractable term $p(z | \mathbf{x}_t)$ in $\mathbf{u}_t(\mathbf{x}_t)$, conditional flow matching (CFM) propose to train the model with an equivalent and tractable conditional objective (Lipman et al., 2023; Tong et al., 2023):

$$\mathcal{L}_{\text{cond}}(\theta) = \mathbb{E}_{t \sim \mathcal{U}(0,1), z \sim p(z), \mathbf{x}_t \sim p_t(\mathbf{x}_t | z)} \left[\left\| \hat{\mathbf{u}}_\theta(\mathbf{x}_t, t) - \mathbf{u}_{t|z}(\mathbf{x}_t | z) \right\|_2^2 \right],$$

whose minimizer coincides with that of conditional loss while remaining simulation-free and easy to estimate.

2.2 LYAPUNOV CONTROL THEORY

To begin with, we consider the feedback-controlled dynamic system of the following general form:

$$\dot{\mathbf{x}} = \mathbf{f}_t(\mathbf{x}, \mathbf{u}(\mathbf{x})), \quad \mathbf{x} \in \mathbb{R}^d, \quad \mathbf{u} \in \mathbb{R}^m, \quad (2)$$

where \mathbf{f}_t is the Lipschitz-continuous vector field acting on some prescribed open set $\mathbf{x} \in \mathcal{D} \subset \mathbb{R}^d$. The solution initiated at time t_0 from \mathbf{x}_0 is denoted by $\mathbf{x}_t(t_0, \mathbf{x}_0)$. We assume that the stationary target position of the controlled system is the origin, i.e. $\mathbf{f}_t(\mathbf{0}, \mathbf{0}) = \mathbf{0}$. One major problem in cybernetics field is to design stabilizing controller $\mathbf{u}(\mathbf{x})$ (Wiener, 2019) such that $\lim_{t \rightarrow \infty} \mathbf{x}_t(t_0, \mathbf{x}_0) = \mathbf{0}$, for any initial value $\mathbf{x}_0 \in \mathcal{D}$.

Theorem 2.1 (Mao, 2007) *Suppose that there exists a continuously differentiable function $V : \mathcal{D} \rightarrow \mathbb{R}$ that satisfies the following conditions: (i) $V(\mathbf{0}) = 0$, (ii) $V(\mathbf{x}) \geq c\|\mathbf{x}\|^p$ for some constants $c, p > 0$, (iii) and $\mathcal{L}_f V < -\delta V$, for some $\delta > 0$.¹ Then, the system is exponentially stable at the origin, that is, $\limsup_{t \rightarrow \infty} \frac{1}{t} \log \|\mathbf{x}(t; t_0, \mathbf{x}_0)\| \leq -\frac{\delta}{p}$. Here V is called a Lyapunov function.*

For a given dynamic system equation 2, the design of appropriate control policies that satisfies the Lyapunov condition in Theorem 2.1 has been a central topic (Chang et al., 2019; Zhang et al., 2022a; Dawson et al., 2023; Yang et al., 2025).

Problem Statement. We assume that flow matching has already learned a base vector field \mathbf{u} transferring the noise distribution p_0 to the data distribution p_1 . For downstream tasks, this vector field must be adapted to generate task-specific conditional distributions $\frac{1}{Z} p_1(\mathbf{x}) e^{-J(\mathbf{x})}$, which is achieved by introducing a Lyapunov function V that encodes task-related priors, and thus the guided field $\mathbf{u} + c$ rigorously samples from the target distribution, where c is a control term derived from V .

There are mainly two scenarios depending on how prior knowledge is provided, which are described in detail as follows.

Scenario 1 (Developers-Oriented). Domain knowledge can be explicitly formulated as an analytical potential $V(\mathbf{x})$, making the conditioning objective transparent.

Typical examples include classifier or classifier-free guidance with class labels (Dhariwal & Nichol, 2021; Ho & Salimans), structural constraints in protein design (Zhang et al., 2024b), and reward functions in reinforcement learning (Janner et al., 2022). Despite their different forms, we provide a unified framework to equate flow matching guidance in Scenario 1 with the Lyapunov control problem (see Section 5.1), and further introduce an efficient and training-free guidance policy grounded in this theoretical framework (see Section 4).

¹ $\mathcal{L}_f V$ represent the Lie derivative of V along the direction \mathbf{f} , i.e., $\mathcal{L}_f V = \nabla V \cdot \mathbf{f}_t$.

Scenario 2 (Users-Oriented). Prior knowledge is implicit and can only be learned through few-shot learning with some data–score pairs $\{(\mathbf{x}_i, V_i)\}_{i=1}^n$, without an explicit conditioner.

In contrast to Scenario 1, the challenge here is to infer a Lyapunov function and corresponding control from sparse or noisy supervision. We address this problem in Section 5.2.

3 A UNIFIED LYAPUNOV GUIDANCE FRAMEWORK FOR FLOW MATCHING

To incorporate diverse forms of prior knowledge into the inference stage of flow matching, we propose a unified Lyapunov guidance framework that interprets guidance as control policy derived from Lyapunov theory. Specifically, we consider the guided vector field as $\mathbf{u}_t + \mathbf{c}_t$, where \mathbf{u}_t is the learned base transport field from noise distribution to data distribution, and \mathbf{c}_t is an auxiliary control term that steers the dynamics toward a conditional target distribution. To align with the common Lyapunov condition, we first introduce *local Lyapunov condition* that formalizes how the controlled dynamics can converge to a desired conditional mode with diverse high-density regions, i.e., attractors. We then propose the first main theorem showing that guided flow matching under unlimited time is equivalent to a Lyapunov control system, with the energy function acting as a Lyapunov function. This equivalence provides a rigorous justification for viewing guidance in generative modeling through the lens of stability theory.

Inspired by Mao (2007), we extend the traditional Lyapunov condition to the following local Lyapunov condition.

Proposition 3.1 (*Local Lyapunov condition*) *For the controlled dynamics $\dot{\mathbf{x}} = \mathbf{u}_t(\mathbf{x}) + \mathbf{c}_t(\mathbf{x})$ under controller $\mathbf{c}_t(\mathbf{x}_t)$, suppose there exists a continuously differentiable function $V : \mathcal{D} \rightarrow \mathbb{R}$ that satisfies the following conditions: (i) for each local minimum point \mathbf{x}^* of V , let $V_{\mathbf{x}^*}(\mathbf{x}) = V(\mathbf{x}) - V(\mathbf{x}^*)$, there exists a ε -neighborhood $O(\mathbf{x}^*, \varepsilon)$ such that $V_{\mathbf{x}^*}(\mathbf{x}) \geq c\|\mathbf{x} - \mathbf{x}^*\|^p, \forall \mathbf{x} \in O(\mathbf{x}^*, \varepsilon)$ for some constants $c, p > 0$, (ii) and $\nabla V(\mathbf{x}) \cdot (\mathbf{u}_t(\mathbf{x}) + \mathbf{c}_t(\mathbf{x})) < -\delta V$, for some $\delta > 0$. Then, the system is locally exponentially stable at \mathbf{x}^* , that is, $\|\mathbf{x}_t - \mathbf{x}^*\| \leq \|\mathbf{x}_0\|e^{-\frac{\delta}{p}t}$. Here V is called a Lyapunov function.*

The above local condition enables us to view the guidance process in flow matching as the synthesis of a stabilizing controller that enforces local convergence toward high-density regions of a target conditional distribution. With this formulation, the energy function commonly used in conditional generative modeling plays the role of a Lyapunov function that shapes the convergence geometry. Our main theorem is presented as follows.

Theorem 3.2 (Equivalence between Guided Flow Matching and Lyapunov Control) *For the flow model $\mathbf{u}_t(\mathbf{x}_t)$ that generates the probability path $p_t(\mathbf{x})$, finding the guidance $\mathbf{c}_t(\mathbf{x}_t)$ to the vector field $\mathbf{u}_t(\mathbf{x}_t)$ to perform conditional sampling $p'_t(\mathbf{x}) = \frac{1}{Z_t}p_t(\mathbf{x})e^{-J(\mathbf{x})}$ is equivalent to finding the controller that satisfies the local Lyapunov condition, where energy function $J(\mathbf{x})$ contributes to Lyapunov function as $V \propto -J$, e.g., $V = -J$.*

The proof is provided in Appendix A.2.1. Theorem 3.2 establishes a general equivalence between conditional generation in flow matching and Lyapunov-based control, where the guidance term acts as a stabilizing controller and the energy (or potential) function plays the role of a Lyapunov function. This theoretical result provides a unified perspective to re-interpret various existing guidance methods in generative modeling as instances of Lyapunov control.

To illustrate the wide applicability of the framework, we identify several representative guidance paradigms where the associated energy function and the conditional distribution naturally serve as Lyapunov functions, so that the guidance terms can be interpreted as controllers that minimize $V(\mathbf{x})$ during generation.

Proposition 3.3 *The following commonly used guidance strategies in generative modeling can all be interpreted as Lyapunov control within our unified framework:*

- **Classifier Guidance:** *Given a trained classifier $p(\mathbf{y}|\mathbf{x})$, the Lyapunov function for guided distribution $p(\mathbf{x}|\mathbf{y})$ specified on conditioner \mathbf{y} is $V_{\mathbf{y}}(\mathbf{x}) = \log p(\mathbf{y}|\mathbf{x})$.*

- **Reward Guidance:** In reinforcement learning tasks with reward function $R(\mathbf{x})$, the Lyapunov function for guided distribution $\frac{1}{Z}p_t(\mathbf{x})e^{R(\mathbf{x})}$ concentrates probability mass in high-reward regions is $V(\mathbf{x}) = -R(\mathbf{x})$.
- **Energy-Based Model (EBM) Guidance:** For a target EBM $p(\mathbf{x}) \propto e^{-E(\mathbf{x})}$, the Lyapunov function is naturally $V(\mathbf{x}) = -E(\mathbf{x})$.
- **Image inverse problems.** Let the forward operator be $\mathbf{y} = H(\mathbf{x}) + \varepsilon$ with $\varepsilon \sim \mathcal{N}(0, \sigma^2 I)$. Then $p(\mathbf{y}|\mathbf{x}) \propto \exp(-\frac{1}{2\sigma^2}\|H(\mathbf{x}) - \mathbf{y}\|_2^2)$ and a natural Lyapunov function is $V_{\mathbf{y}}(\mathbf{x}) = \frac{1}{2\sigma^2}\|H(\mathbf{x}) - \mathbf{y}\|_2^2$, yielding guided sampling $p'_t(\mathbf{x}) \propto p_t(\mathbf{x}) \exp(-V_{\mathbf{y}}(\mathbf{x}))$ that enforces data consistency Song et al. (2023).

In Appendix A.2.2, we provide proof of the proposition and further discuss the relationship between exiting guidance methods and our framework.

Variants of LyaGuide. The Proposition 3.1 establishes exponential stability of the controlled system, so we denote the corresponding method as **LyaGuide-ES**. Under a weaker condition that $\delta = 0$ in Theorem 3.2, the equilibrium remains stable in the sense of asymptotic stability, i.e., $\lim_{t \rightarrow \infty} \|\mathbf{x}_t - \mathbf{x}^*\| = 0$. In this case, V is also a valid Lyapunov function. In addition, we can also modify the Lyapunov condition for a stronger exponential convergence. Therefore, two natural variants of LyaGuide arise by either relaxing or strengthening the Lyapunov condition:

- **LyaGuide-AS (Asymptotic Stability).** Setting $\delta = 0$ reduces the condition to $\nabla V(\mathbf{x}) \cdot (\mathbf{u}_t(\mathbf{x}) + \mathbf{c}_t(\mathbf{x})) < 0$, which guarantees asymptotic convergence $\lim_{t \rightarrow \infty} \|\mathbf{x}_t - \mathbf{x}^*\| = 0$. This yields a weaker but broadly applicable guidance mechanism.
- **LyaGuide-CS (Component-wise Stability).** A stronger requirement is that each component marked by subscript i satisfies $\nabla V(\mathbf{x})_i(\mathbf{u}_t(\mathbf{x}) + \mathbf{c}_t(\mathbf{x}))_i \leq -\delta V(\mathbf{x})$. This enforces descent along all directions and provides stricter stability guarantees for the guided flow.

These two variants offer flexible trade-offs between stability and practical applicability. Empirically, LyaGuide-ES and LyaGuide-CS demonstrate superior performance and greater robustness across tasks, and we therefore recommend them as the default variants in practice (see Appendix A.5).

4 PSEUDO PROJECTION OPERATION FOR LYAPUNOV GUARANTEE

Given the equivalence between the guided flow matching and Lyapunov control, we show how we can better design the guidance term from the perspective of Lyapunov principle. Before the introduction of Lyapunov guidance, we propose a novel pseudo projection method that efficiently corrects the guidance term learned by neural networks. As in neural control, the candidate guidance function in flow may not rigorously satisfy the Lyapunov condition across the entire state space, since it is often learned from finite data or heuristically constructed. To address this limitation, we propose a projection operator that enforces the Lyapunov condition by projecting any candidate guidance into the admissible set of Lyapunov-stable controls.

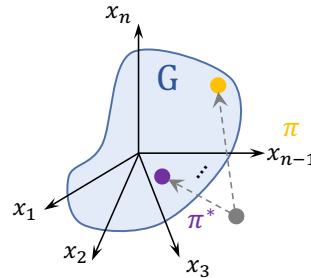


Figure 2: Illustration of the pseudo projection, G represents the target guidance space.

Theorem 4.1 (Lyapunov Guarantee for Guidance)

For a candidate controller c and the guidance controller space $\mathcal{U}(V) = \{\mathbf{u} : \nabla V \cdot (\mathbf{u}_t + \mathbf{c}_t) + \delta V \leq 0\}$ that rigorously satisfies the local Lyapunov condition in Proposition 3.1, define the projection operator as

$$\pi(\mathbf{c}_t, \mathcal{U}(V)) \triangleq \mathbf{c}_t - \frac{\max(0, \nabla V(\mathbf{x}) \cdot (\mathbf{u}_t(\mathbf{x}) + \mathbf{c}_t(\mathbf{x})) + \delta V(\mathbf{x}))}{\|\nabla V(\mathbf{x})\|^2} \nabla V(\mathbf{x}).$$

Then $\pi(\mathbf{c}_t, \mathcal{U}(V))$ is locally Lipschitz continuous and thus the guided flow under $\pi(\mathbf{c}_t, \mathcal{U}(V))$ is well defined, and $\pi(\mathbf{c}_t, \mathcal{U}(V)) \in \mathcal{U}(V)$.

The proof is provided in Appendix A.2.3. Fig. 2 shows the idea behind the pseudo projection, that any candidate guidance function can be systematically corrected via the pseudo projection operation,

yielding a valid Lyapunov guidance that rigorously satisfies the stability condition across the state space. Therefore, our approach enjoys theoretical guarantees of conditional sampling via Lyapunov stability even when the initial candidate does not. Combining Theorem 3.2 with Theorem 4.1, we obtain a rigorous guarantee that flow model with projected guidance rigorously converges to the target distribution.

Exact Projection vs. Pseudo Projection. We refer to the operator in Theorem 4.1 as a *pseudo projection*, because for a feedback controller \mathbf{c} , it is not the exact solution of the classical projection problem Deenen et al. (2021):

$$\begin{aligned} \pi^*(\mathbf{c}) &\in \arg \min_{\tilde{\mathbf{c}}} \|\mathbf{c} - \tilde{\mathbf{c}}\|_{C(\mathbb{R}^d)}, \\ \text{s.t. } \nabla V(\mathbf{x}) \cdot (\mathbf{u}_t(\mathbf{x}) + \mathbf{c}(\mathbf{x})) &\leq -\delta V, \quad \forall \mathbf{x} \in \mathcal{D}. \end{aligned}$$

In general, obtaining a closed-form expression of the exact projection operator π is intractable. A common alternative is to solve a simplified quadratic program (QP) at each state \mathbf{x} Chow et al. (2019):

$$\begin{aligned} \tilde{\pi}(\mathbf{c})(\mathbf{x}) &\in \arg \min_{\tilde{\mathbf{c}}(\mathbf{x})} \|\mathbf{c}(\mathbf{x}) - \tilde{\mathbf{c}}(\mathbf{x})\|, \\ \text{s.t. } \nabla V(\mathbf{x}) \cdot (\mathbf{u}_t(\mathbf{x}) + \mathbf{c}(\mathbf{x})) &\leq -\delta V(\mathbf{x}). \end{aligned}$$

Although this guarantees the Lyapunov condition for each state \mathbf{x} , it requires solving an online optimization problem. In the context of flow matching, the dimensionality of the state space can be very high (e.g., images, molecular structures, or protein conformations). In such cases, solving a QP in every integration step would be prohibitively expensive. In contrast, the pseudo projection in Theorem 4.1 has an explicit analytical form, making it more efficient in practice while still ensuring that the guidance satisfies the Lyapunov condition.

In the context of flow matching, the dimensionality of the state space can be very high (e.g., images, molecular structures, or protein conformations). In such cases, solving a QP in each integration step would be prohibitively expensive. The pseudo projection offers a tractable alternative with closed-form updates, enabling stability enforcement during sampling without introducing substantial computational overhead. This makes the proposed approach particularly well suited for high-dimensional generative modeling tasks.

5 LYAPUNOV GUIDANCE FOR DIFFERENT SCENARIOS

Building on the equivalence between guided flow matching and Lyapunov control that established in Section 3, we now specify the guidance policies for two different practical scenarios. The distinction lies in whether prior knowledge can be explicitly formulated: in Scenario 1, the Lyapunov function V admits an analytical expression, and guidance can be synthesized directly (or learned from V); but in Scenario 2, the Lyapunov function is unknown and must be learned from data, which requires us to learn both V and the associated control.

5.1 SCENARIO 1: EXPLICIT PRIOR KNOWLEDGE

When domain knowledge can be analytically represented, the Lyapunov function $V(\mathbf{x})$ is directly available. For such tasks, $V(\mathbf{x})$ acts as a certificate function that encodes domain-specific constraints, while the control term $\mathbf{c}(\mathbf{x}, t)$ is designed according to the Lyapunov condition in Proposition 3.1, ensuring that the guided flow is exponentially stable toward the high-density regions of the conditional distribution.

According to the projection operation described in Section 4, we begin with a candidate guidance function and then enforce the Lyapunov condition by projecting it onto the admissible function space. Within the flow matching literature, a common choice of candidate is based on the gradient of the Lyapunov function, $\mathbf{c}_t(\mathbf{x}) \propto -\nabla V(\mathbf{x})$, which is closely related to the score function of the prior energy distribution Song & Ermon (2019). The complete procedure is summarised in Algorithm 1.

5.2 SCENARIO 2: IMPLICIT PRIOR KNOWLEDGE VIA FEW-SHOT LEARNING

When explicit formulations of prior knowledge are unavailable, we assume access to a small set of preference data–score pairs $\{(\mathbf{x}_i, V_i)\}_{i=1}^n$, where V_i represents a task-specific score or energy eval-

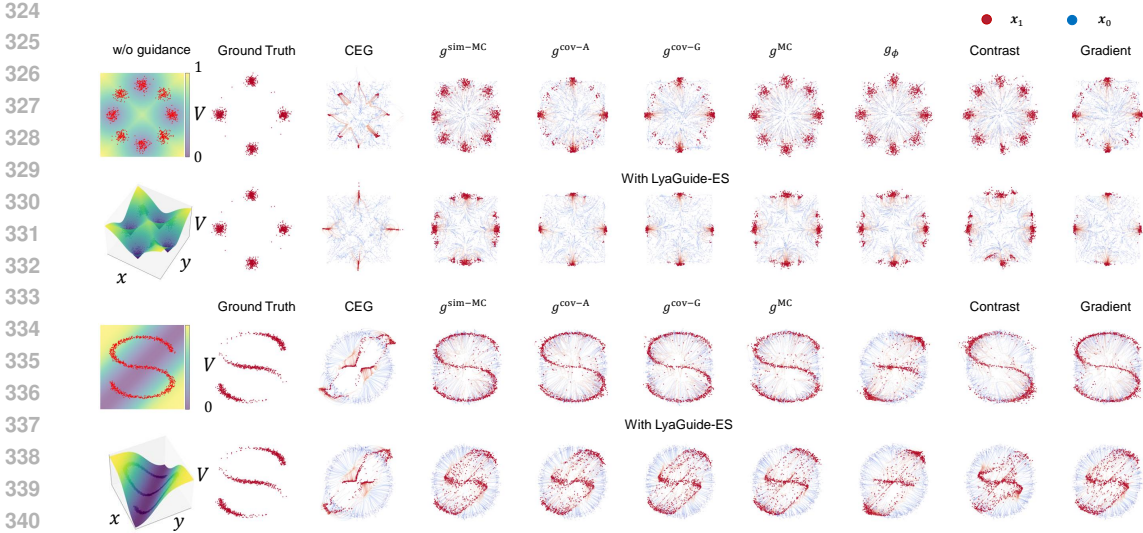


Figure 3: Scenario 1 results on synthetic dataset. For each target distribution, the top (resp. bottom) row correspond to the methods without (resp. with) LyaGuide. We visualize the start/end points and the flow trajectories. LyaGuide significantly improves the performance across different methods.

uated at x_i . Our first goal is to recover a Lyapunov function $V_{\theta_V}(\mathbf{x})$ from these pairs by minimizing a supervised regression loss: $\mathcal{L}_V(\theta_V) = \frac{1}{n} \sum_{i=1}^n (V_{\theta_V}(\mathbf{x}_i) - V_i)^2$.

Convexity-aware training of V . Proposition 3.1 requires V to be locally convex around task-relevant regions. To bias the learner toward such regions when only few-shot supervision (\mathbf{x}_i, V_i) is available, we adopt a soft importance weighting on the targets, $w_i = \frac{\exp(-\alpha V_i)}{\sum_{j=1}^n \exp(-\alpha V_j)}$, which emphasizes lower-score samples (closer to local minima) and thus promotes convexity where it matters. We then estimate V_{θ_V} via a weighted regression augmented with a convexity regularizer:

$$\mathcal{L}_V(\theta_V) = \frac{1}{n} \sum_{i=1}^n w_i (V_{\theta_V}(\mathbf{x}_i) - V_i)^2. \tag{3}$$

Control design. Once a valid Lyapunov function V_{θ_V} is obtained, the corresponding guidance control can then be derived in two ways: either by explicit synthesis according to the Lyapunov framework,

$$\mathbf{c}(\mathbf{x}, t) = \arg \min_{\mathbf{c}} \nabla V_{\theta_V}(\mathbf{x}) \cdot (\mathbf{u}_t(\mathbf{x}) + \mathbf{c}(\mathbf{x}, t)) + \delta V_{\theta_V}(\mathbf{x}),$$

or by integrating V_{θ_V} into existing guidance methods (e.g. classifier or reward guidance) to regularize their dynamics via a Lyapunov-inspired penalty. In this work we employ the training algorithm g_ϕ posed in Feng et al. (2025) for learning the guidance.

This two-stage design separates the estimation of the implicit energy landscape from the design of the guidance control, enabling user-provided supervision to be incorporated flexibly into flow matching. Although we present a two-stage procedure here (first learning V , then designing \mathbf{c}), in practice V and \mathbf{c} can also be optimized jointly under a Lyapunov-inspired loss, as applied in Zhang et al. (2022a; 2024a); Yang et al. (2025)

6 EXPERIMENTS

In this section, we demonstrate the superiority of the LyaGuide over existing methods with extensive experiments from low dimensional tasks to high dimensional tasks. More details of the experiments can be found in Appendix A.5.

6.1 EVALUATION ON SYNTHETIC DATASET

Scenario 1: We first evaluate our approach on the synthetic datasets introduced in (Feng et al., 2025), where the source distribution p_0 is chosen as uniform (resp. circle) distribution and the target distribution p_1 is an 8-Gaussian mixture (resp. S-curve). For each dataset, we design a task-specific energy function V to encode prior knowledge, as shown in Fig. 3 (first column on the left).

We compare against a wide range of existing guidance methods reported in Feng et al. (2025) as our baseline: contrastive energy guidance (CEG) Lu et al. (2023), Monte Carlo guidance (g^{MC}), learned guidance (g_ϕ), covariance-based approximations ($g^{\text{cov-A}}$ and $g^{\text{cov-G}}$), and simplified Monte Carlo ($g^{\text{sim-MC}}$). We also include contrastive guidance, which drives the flow toward unexpected regions, and gradient-based guidance commonly used in generative modeling Zhang et al. (2024b) for comparison. Each of these methods is first applied in its original form, and then we treat their guidance terms as candidates in Algorithm 1 and refine them with our proposed LyaGuide-ES. We also provide some detailed analysis results for LyaGuide-AS and LyaGuide-CS in Appendix A.5.

As shown in Fig. 3, all methods benefit from our Lyapunov guidance, where the guided trajectories become more stable and align more closely with the ground truth distribution. Specifically, for the first task (8-Gaussian mixture), we can see that most of the methods fail to sample correct trajectories without the guidance of LyaGuide, of which the best performance achieved by $g^{\text{cov-A}}$, $g^{\text{cov-G}}$ and *Gradient* is still defective, while noise at the four corners of the diagonals drops off drastically or even disappears after application of LyaGuide. Similar effect can be observed for the second task (S-curve distribution), where the LyaGuide optimized methods exhibit sharper mode coverage and fewer spurious samples compared to the original versions. These results demonstrate that LyaGuide provides an effective and practical way to improve guidance quality, consistently achieving gains across all baselines and energy functions.

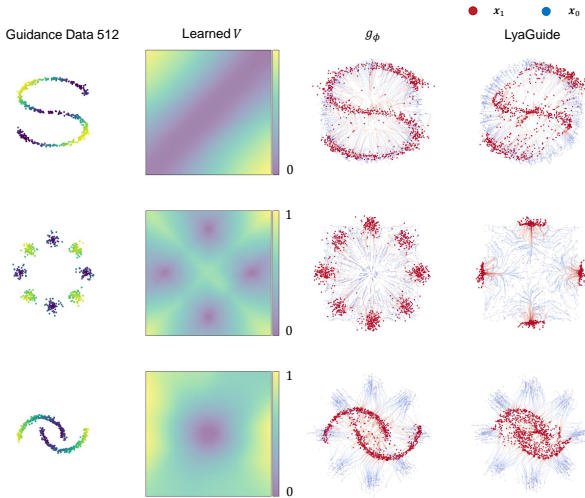


Figure 4: Scenario 2 results with dataset size = 512.

Boundary effects of Pseudo Projection. We also note that there are two subtleties in the second task. First, CEG+Lya shows little difference with CEG, as the original samples already lie in the trough of V ; since our projection encourages trajectories toward the trough, no further adjustment occurs. Second, Contrast+Lya does not preserve the exact masked S-curve shape. Instead, samples concentrate along the boundary of the trough of V , consistent with our projection principle: enforcing the Lyapunov inequality $\{\mathbf{x} : \nabla V(\mathbf{x}) \cdot (\mathbf{u}_t(\mathbf{x}) + \mathbf{c}_t(\mathbf{x})) \leq -\delta V(\mathbf{x})\}$. Thus, data near the peaks of V are guided toward the nearest trough boundary, rather than the lower-left or upper-right arms of the S-curve.

Scenario 2: We next evaluate LyaGuide in Scenario 2, where explicit prior knowledge is not available and only a small set of preference data–score pairs is provided. Following the setup in Section 5.2, we learn a Lyapunov function V_{θ_V} first and then derive the guidance control either through explicit synthesis or by integrating into existing methods. We consider synthetic benchmarks with three tasks, and vary the number of supervision pairs $\{(\mathbf{x}_i, V_i)\}$ from 128 to 1024.

As shown in Fig. 4, even with very sparse supervision, LyaGuide successfully recovers meaningful Lyapunov landscapes whose minima align with the high-density regions of the target distribution. Compared to the baseline g_ϕ , the LyaGuide method enforces stability throughout the trajectory, yielding better guided flows that concentrate around the correct modes while suppressing spurious samples. We further perform the ablation study on data size in Appendix A.5.

6.2 IMAGE INVERSE PROBLEMS

We further validate LyaGuide on high-dimensional image inverse problems, which have become a standard benchmark for assessing guidance quality in flow matching (Song et al., 2023; Feng et al., 2025). The objective is to reconstruct a clean image x from a corrupted observation $y = H(x) + \varepsilon$, where H is a known degradation operator and ε denotes Gaussian noise. In contrast to pseudoinverse-guided diffusion (Song et al., 2023), our projection-based scheme offers a lightweight alternative that strictly enforces stability during sampling.

We evaluate on the CelebA-HQ dataset under the box inpainting setting, where a central square region of each image is masked and the model must complete the missing content. Performance is measured by FID, LPIPS, PSNR, and SSIM on 3000 test samples. As summarized in Table 1, LyaGuide consistently improves all baseline guidance methods. Similar improvements are also observed on two additional inverse problems, namely super-resolution and Gaussian deblurring, with detailed comparisons reported in Appendix A.5.

Table 1: Image inverse problem results on CelebA-HQ (Box painting task). The best and runner-up results are highlighted with **bold** and underline, respectively.

		Original Methods				LyaGuide-ES				LyaGuide-CS			
		FID ↓	LPIPS ↓	PSNR ↑	SSIM ↑	FID ↓	LPIPS ↓	PSNR ↑	SSIM ↑	FID ↓	LPIPS ↓	PSNR ↑	SSIM ↑
OT-CFM	$g^{\text{cov-A}}$	<u>7.3387</u>	0.1907	25.5984	0.8431	7.4039	<u>0.1898</u>	25.6935	<u>0.8442</u>	6.4722	0.1739	25.6217	0.8562
	$g^{\text{sim-A}}$	19.8569	0.2309	<u>26.4127</u>	0.7950	19.8852	0.2309	26.4741	0.7950	12.7344	0.1921	26.3142	0.842
	IIGDM	30.3839	0.3200	20.8253	0.7193	30.3839	0.3200	20.8253	0.7193	26.785	0.291	21.3654	0.7473
	g^{MC}	18.6635	0.2391	26.9492	0.8124	24.1950	0.2396	26.9624	0.8129	16.0392	0.2283	27.0681	0.8200
CFM	$g^{\text{cov-A}}$	7.6629	0.1922	25.8612	0.8414	7.6819	0.1918	25.9367	0.8419	<u>6.9783</u>	<u>0.1764</u>	25.8155	0.854
	$g^{\text{sim-A}}$	9.7060	0.1935	26.0867	0.8263	9.6002	0.1935	26.1094	0.8263	6.8763	0.1629	26.0592	<u>0.8508</u>
	$g^{\text{cov-G}}$	19.8022	0.2379	<u>27.0087</u>	0.8138	24.3271	0.2379	27.0017	0.8145	22.0999	0.2293	27.0301	0.8206
	IIGDM	19.0847	0.2323	25.6418	0.8093	19.0619	0.2336	25.9002	0.8074	14.1461	0.2003	26.112	0.8439

7 SCOPE AND LIMITATIONS

Finite-Time Lyapunov Control. Our framework currently relies on asymptotic Lyapunov stability, which ensures convergence as $t \rightarrow \infty$ but does not provide accurate convergence time for Lyapunov control. Since generative models operate with fixed inference time, a natural question is whether finite-time or prescribed-time Lyapunov control can be incorporated to regulate convergence within this horizon. While classical finite-time theory (Polyakov, 2012; Polyakov et al., 2015) guarantees bounded-time stability, its direct use may neglect the data distribution $p_1(x) = q(x)$. Future work could therefore explore finite-time Lyapunov methods or design distribution-level Lyapunov functionals that couple $q(x)$ with the task-specific energy $J(x)$, enabling faithful generation with controlled convergence speed.

On the Role of the Potential V . Our guarantees hinge on the availability or learnability of a potential V that meaningfully encodes task priors. When V is poorly specified or underfitted, guidance may bias samples toward suboptimal regions, a limitation shared with classifier/EBM/reward guidance in diffusion (Dhariwal & Nichol, 2021; Ho & Salimans; Janner et al., 2022). Scenario 2 mitigates this by learning V_θ from few-shot supervision with a Lyapunov penalty, but the expressiveness-regularity trade-off remains: overly flexible V_θ may violate smoothness or curvature required for stabilization and overly rigid V_θ may underfit complex priors, how to address such issue in learning Lyapunov function is a future research direction.

8 CONCLUSION

In this work, we introduce LyaGuide, a unified framework that reformulates guidance in flow matching as a Lyapunov control problem. By establishing a theoretical equivalence between guided flows and Lyapunov stabilization control process, we show that diverse guidance strategies can be interpreted within a single control-theoretic perspective. To rigorously enforce stability, we also propose a pseudo projection operator with a closed-form expression, which guarantees that any candidate guidance satisfies the Lyapunov condition. Notably, this projection can be implemented with a single line of code and is compatible with existing guidance methods, consistently enhancing their performance. This work opens new opportunities for control-inspired generative modeling, particularly in domains where explicit priors are scarce but limited supervision can be leveraged, making the framework especially suitable for deploying pre-trained models on individual systems.

486 REPRODUCIBILITY STATEMENT
487

488 The code of the experiments used in this paper is available at:
489 https://anonymous.4open.science/r/LyaGuide_ICLR2026-F3BB, and com-
490 plete proofs of our theoretical claims can be found in Appendix A.2.
491

492 REFERENCES
493

494 M. S. Albergo, M. Rizzi, and K. Cranmer. Stochastic interpolant: A new framework for generative
495 modeling. In *International Conference on Machine Learning (ICML)*, 2023.
496

497 Zvi Artstein. Stabilization with relaxed controls. *Nonlinear Analysis: Theory, Methods & Applica-*
498 *tions*, 7(11):1163–1173, 1983.

499 Kevin Black, Michael Janner, Yilun Du, Ilya Kostrikov, and Sergey Levine. Training diffusion
500 models with reinforcement learning. In *The Twelfth International Conference on Learning Rep-*
501 *resentations*, 2023.
502

503 Ya-Chien Chang, Nima Roohi, and Sicun Gao. Neural lyapunov control. In *Proceedings of the 33rd*
504 *International Conference on Neural Information Processing Systems*, pp. 3245–3254, 2019.
505

506 T. Chen, J. Gu, and L. Dinh. Generative modeling with phase stochastic bridges. In *International*
507 *Conference on Learning Representations (ICLR)*, 2023.

508 Yinlam Chow, Ofir Nachum, Aleksandra Faust, Edgar Duenez-Guzman, and Mohammad
509 Ghavamzadeh. Lyapunov-based safe policy optimization for continuous control. *arXiv preprint*
510 *arXiv:1901.10031*, 2019.
511

512 Charles Dawson, Sicun Gao, and Chuchu Fan. Safe control with learned certificates: A survey of
513 neural lyapunov, barrier, and contraction methods for robotics and control. *IEEE Transactions on*
514 *Robotics*, 2023.

515 Daniel Andreas Deenen, Bardia Sharif, Sebastiaan van den Eijnden, Hendrik Nijmeijer, Maurice
516 Heemels, and Marcel Heertjes. Projection-based integrators for improved motion control: For-
517 malization, well-posedness and stability of hybrid integrator-gain systems. *Automatica*, 133:
518 109830, 2021.
519

520 Prafulla Dhariwal and Alexander Nichol. Diffusion models beat gans on image synthesis. *Advances*
521 *in neural information processing systems*, 34:8780–8794, 2021.

522 T. Dockhorn, A. Vahdat, and K. Kreis. Score-based generative modeling in latent space. In *Advances*
523 *in Neural Information Processing Systems (NeurIPS)*, 2022.
524

525 Yilun Du and Igor Mordatch. Implicit generation and modeling with energy based models. *Advances*
526 *in neural information processing systems*, 32, 2019.

527 Weichen Fan, Amber Yijia Zheng, Raymond A Yeh, and Ziwei Liu. Cfg-zero*: Improved classifier-
528 free guidance for flow matching models. *CoRR*, 2025.
529

530 Ruiqi Feng, Chenglei Yu, Wenhao Deng, Peiyan Hu, and Tailin Wu. On the guidance of flow
531 matching. In *Forty-second International Conference on Machine Learning*, 2025.
532

533 Chelsea Finn, Pieter Abbeel, and Sergey Levine. Model-agnostic meta-learning for fast adaptation
534 of deep networks. In *ICML*, 2017.

535 Jonathan Ho and Tim Salimans. Classifier-free diffusion guidance. In *NeurIPS 2021 Workshop on*
536 *Deep Generative Models and Downstream Applications*.
537

538 Michael Janner, Yilun Du, Joshua Tenenbaum, and Sergey Levine. Planning with diffusion for
539 flexible behavior synthesis. In *International Conference on Machine Learning*, pp. 9902–9915.
PMLR, 2022.

- 540 Qiyu Kang, Yang Song, Qinxu Ding, and Wee Peng Tay. Stable neural ode with lyapunov-stable
541 equilibrium points for defending against adversarial attacks. *Advances in Neural Information*
542 *Processing Systems*, 34:14925–14937, 2021.
- 543 Hassan K Khalil. Nonlinear systems third edition. *Patience Hall*, 115, 2002.
- 544 Yann LeCun, Sumit Chopra, Raia Hadsell, M Ranzato, Fugie Huang, et al. A tutorial on energy-
545 based learning. *Predicting structured data*, 1(0), 2006.
- 546 Kyungmin Lee, Xiahong Li, Qifei Wang, Junfeng He, Junjie Ke, Ming-Hsuan Yang, Irfan Essa,
547 Jinwoo Shin, Feng Yang, and Yinxiao Li. Calibrated multi-preference optimization for aligning
548 diffusion models. In *Proceedings of the Computer Vision and Pattern Recognition Conference*,
549 pp. 18465–18475, 2025.
- 550 Yaron Lipman, Ricky TQ Chen, Heli Ben-Hamu, Maximilian Nickel, and Matt Le. Flow matching
551 for generative modeling. In *11th International Conference on Learning Representations, ICLR*
552 *2023*, 2023.
- 553 J. Liu, Y. Meng, and M. Fitzsimmons. Physics-informed neural network lyapunov functions: Pde
554 characterization, learning, and verification. *Journal of Machine Learning Research*, 24(210):
555 1–36, 2023a.
- 556 Xingchao Liu, Chengyue Gong, et al. Flow straight and fast: Learning to generate and transfer
557 data with rectified flow. In *The Eleventh International Conference on Learning Representations*,
558 2023b.
- 559 Cheng Lu, Huayu Chen, Jianfei Chen, Hang Su, Chongxuan Li, and Jun Zhu. Contrastive energy
560 prediction for exact energy-guided diffusion sampling in offline reinforcement learning. In *Inter-*
561 *national Conference on Machine Learning*, pp. 22825–22855. PMLR, 2023.
- 562 Xuerong Mao. *Stochastic differential equations and applications*. Elsevier, 2007.
- 563 Pablo A Parrilo. *Structured Semidefinite Programs and Semialgebraic Geometry Methods in Ro-*
564 *bustness and Optimization*. California Institute of Technology, 2000.
- 565 Andrey Polyakov. Nonlinear feedback design for fixed-time stabilization of linear control systems.
566 *IEEE Transactions on Automatic Control*, 57(8):2106–2110, 2012.
- 567 Andrey Polyakov, Denis Efimov, and Wilfrid Perruquetti. Finite-time and fixed-time stabilization:
568 Implicit lyapunov function approach. *Automatica*, 51:332–340, 2015.
- 569 Zengyi Qin, Kaiqing Zhang, Yuxiao Chen, Jingkai Chen, and Chuchu Fan. Learning safe multi-agent
570 control with decentralized neural barrier certificates. In *International Conference on Learning*
571 *Representations*, 2020.
- 572 Sylvestre-Alvise Rebuffi, Hakan Bilen, and Andrea Vedaldi. Learning multiple visual domains with
573 residual adapters. In *NeurIPS*, 2017.
- 574 Andrei A Rusu, Dushyant Rao, Jakub Sygnowski, Razvan Pascanu, Simon Osindero, and Raia
575 Hadsell. Meta-learning with latent embedding optimization. In *ICLR*, 2019.
- 576 Jiaming Song, Arash Vahdat, Morteza Mardani, and Jan Kautz. Pseudoinverse-guided diffusion
577 models for inverse problems. In *International Conference on Learning Representations*, 2023.
- 578 Yang Song and Stefano Ermon. Generative modeling by estimating gradients of the data distribution.
579 *Advances in neural information processing systems*, 32, 2019.
- 580 Yang Song, Jascha Sohl-Dickstein, Diederik P. Kingma, Abhishek Kumar, Stefano Ermon, and Ben
581 Poole. Score-based generative modeling through stochastic differential equations. In *Intern-*
582 *ational Conference on Learning Representations*, 2021.
- 583 Eduardo D Sontag. A ‘universal’ construction of artstein’s theorem on nonlinear stabilization. *Sys-*
584 *tems & control letters*, 13(2):117–123, 1989.

- 594 Christopher Iliffe Sprague, Arne Elofsson, and Hossein Azizpour. Incorporating stability into flow
595 matching. In *ICML 2024 Workshop on Structured Probabilistic Inference & Generative Mod-*
596 *eling*, 2024.
- 597 Dawei Sun, Susmit Jha, and Chuchu Fan. Learning certified control using contraction metric. In
598 *Conference on Robot Learning*, pp. 1519–1539. PMLR, 2021.
- 600 Alexander Tong, Nikolay Malkin, Guillaume Huguette, Yanlei Zhang, Jarrid Rector-Brooks, Kilian
601 Fatras, Guy Wolf, and Yoshua Bengio. Conditional flow matching: Simulation-free dynamic
602 optimal transport. *arXiv preprint arXiv:2302.00482*, 2(3), 2023.
- 603 Hiroyasu Tsukamoto, Soon-Jo Chung, and Jean-Jaques E Slotine. Contraction theory for nonlinear
604 stability analysis and learning-based control: A tutorial overview. *Annual Reviews in Control*, 52:
605 135–169, 2021.
- 607 Norbert Wiener. *Cybernetics or Control and Communication in the Animal and the Machine*. MIT
608 press, 2019.
- 609 Luan Yang, Jingdong Zhang, Qunxi Zhu, and Wei Lin. Neural event-triggered control with optimal
610 scheduling. *arXiv preprint arXiv:2507.14653*, 2025.
- 612 Hengtong Zhang and Tingyang Xu. Towards controllable diffusion models via reward-guided ex-
613 ploration. *arXiv preprint arXiv:2304.07132*, 2023.
- 614 Jingdong Zhang, Qunxi Zhu, and Wei Lin. Neural stochastic control. In *Advances in Neural Infor-*
615 *mation Processing Systems*, 2022a.
- 617 Jingdong Zhang, Qunxi Zhu, Wei Yang, and Wei Lin. Sync: Safety-aware neural control for stabiliz-
618 ing stochastic delay-differential equations. In *The Eleventh International Conference on Learning*
619 *Representations*, 2022b.
- 620 Jingdong Zhang, Luan Yang, Qunxi Zhu, and Wei Lin. Fessnc: Fast exponentially stable and safe
621 neural controller. In *International Conference on Machine Learning*, pp. 60076–60098. PMLR,
622 2024a.
- 624 Zaixi Zhang, Marinka Zitnik, and Qi Liu. Generalized protein pocket generation with prior-informed
625 flow matching. *Advances in neural information processing systems*, 37:38559–38589, 2024b.
- 626
627
628
629
630
631
632
633
634
635
636
637
638
639
640
641
642
643
644
645
646
647

A APPENDIX

A.1 ALGORITHMS

Algorithm 1: LyaGuide: Training-free Approach

-
- 1: **Input:** Learned vector field u_t in flow matching, explicit Lyapunov function $V(x)$ for prior knowledge, guidance parameter δ , initial parameter set k .
 - 2: **Candidate guidance:** E.g., $c_t(\mathbf{x}) = -k\nabla V(\mathbf{x})$ ▷ user-defined
 - 3: **Pseudo projection operation** for rigorous satisfaction of Lyapunov condition 3.1:
 - 4: **LyaGuide-ES:** $c_t^*(\mathbf{x}) = c_t(\mathbf{x}) - \frac{\max(0, \nabla V \cdot (\mathbf{u}_t + c_t) + \delta V)}{\|\nabla V\|^2} \cdot \nabla V$
 - 5: **LyaGuide-AS:** $c_t^*(\mathbf{x}) = c_t(\mathbf{x}) - \frac{\max(0, \nabla V \cdot (\mathbf{u}_t + c_t))}{\|\nabla V\|^2} \cdot \nabla V$
 - 6: **LyaGuide-CS:** $c_t^*(\mathbf{x})_i = (c_{\theta_c}(\mathbf{x}, t))_i - \frac{\max(0, (\nabla V)_i(\mathbf{u} + c)_i + \delta V)}{\|\nabla V\|^2} \cdot \nabla V$
 - 7: **Output:** Guided vector field $\mathbf{f}_t(\mathbf{x}) = \mathbf{u}_t(\mathbf{x}) + c_t^*(\mathbf{x})$ for conditional flow matching.
-

The score-based candidate guidance in Algorithm 1 provides an efficient approximation to the ideal guidance, although its performance depends on the choice of the initial parameter k . A better candidate may be obtained by iteratively running the algorithm with different values of k and selecting the best outcome. More generally, any other method for generating a guidance term can be seamlessly integrated into our framework Feng et al. (2025). In particular, one may train a neural network to approximate the candidate guidance, as we demonstrate in Scenario 2 below.

Algorithm 2: LyaGuide: Training-based Approach

-
- Input:** Preference data-score pairs $\mathcal{D} = \{(\mathbf{x}_i, V_i)\}_{i=1}^n$, learning rate β , initial parameters θ_0 , $\theta = (\theta_V, \theta_c)$, learned flow \mathbf{u}_t from take noisy distribution p_0 to data distribution p_1 , guidance parameter δ .
- while not converged do**
- $(\mathbf{x}_i, V_i) \sim \mathcal{D}$ ▷ sample data and score
 - Compute Lyapunov Loss $L(\theta_V)$ from equation 3
 - $\theta_V \leftarrow \theta_V - \beta \nabla_{\theta} L(\theta_V)$ ▷ Learn Lyapunov function
 - Train θ_c with any existing learning-based guidance method
- Pseudo projection operation :**
- LyaGuide-ES:** $c_t^*(\mathbf{x}) = c_{\theta_c}(\mathbf{x}, t) - \frac{\max(0, \nabla V_{\theta_V} \cdot (\mathbf{u} + c) + \delta V_{\theta_V})}{\|\nabla V_{\theta_V}\|^2} \cdot \nabla V_{\theta_V}$
- LyaGuide-AS:** $c_t^*(\mathbf{x}) = c_{\theta_c}(\mathbf{x}, t) - \frac{\max(0, \nabla V_{\theta_V} \cdot (\mathbf{u} + c))}{\|\nabla V_{\theta_V}\|^2} \cdot \nabla V_{\theta_V}$
- LyaGuide-CS:** $c_t^*(\mathbf{x})_i = (c_{\theta_c}(\mathbf{x}, t))_i - \frac{\max(0, (\nabla V_{\theta_V})_i(\mathbf{u} + c)_i + \delta V_{\theta_V})}{\|\nabla V_{\theta_V}\|^2} \cdot \nabla V_{\theta_V}$
- Output:** Guided vector field $\mathbf{f}_t(\mathbf{x}) = \mathbf{u}_t(\mathbf{x}) + c_t^*(\mathbf{x})$ for conditional flow matching.
-

A.2 THEORETICAL PROOFS

Notations. Denote by $\|\cdot\|$ the L^2 -norm for any given vector in \mathbb{R}^d . Denote by $\|\cdot\|_{C(\mathcal{D})}$ the maximum norm on continuous function space $C(\mathcal{D})$. For $A = (a_{ij})$, a matrix of dimension $d \times r$, denote by $\|A\|_F^2 = \sum_{i=1}^d \sum_{j=1}^r a_{ij}^2$ the Frobenius norm. Denote $\max(a, 0)$ by $(a)^+$. Denote $\mathbf{x} \cdot \mathbf{y}$ as the inner product of two vectors.

A.2.1 PROOF OF THEOREM 3.2

Theorem A.1 (Equivalence between Guided Flow Matching and Lyapunov Control) *For the VF $\mathbf{u}_t(\mathbf{x}_t)$ that generates the probability path $p_t(\mathbf{x})$, finding the guidance $c_t(\mathbf{x}_t)$ to the vector field $\mathbf{u}_t(\mathbf{x}_t)$ to perform conditional sampling $p_t^*(\mathbf{x}) = \frac{1}{Z_t} p_t(\mathbf{x}) e^{-J(\mathbf{x})}$ is equivalent to finding the controller that satisfies the local Lyapunov condition, where energy function $J(\mathbf{x})$ contributes to Lyapunov function as $V \propto -J$, e.g., $\dot{V} = -J$.*

Proof. Let p_t be the probability path governed by the continuity equation

$$\partial_t p_t(\mathbf{x}) + \nabla \cdot (p_t(\mathbf{x}) \mathbf{u}_t(\mathbf{x})) = 0, \quad (4)$$

where \mathbf{u}_t is the trained flow model. For energy $J(\mathbf{x})$, define the reweighted path as

$$p'_t(\mathbf{x}) = \frac{1}{Z_t} e^{-J(\mathbf{x})} p_t(\mathbf{x}), \quad Z_t = \int e^{-J(\mathbf{x})} p_t(\mathbf{x}) d\mathbf{x}. \quad (5)$$

We assume sufficient smoothness, and either periodic boundary conditions or vanishing flux at infinity so that boundary integrals of divergences vanish.

Step 1. By definition equation 5 we have,

$$\begin{aligned} \partial_t p'_t &= \partial_t \left(\frac{e^{-J}}{Z_t} p_t \right) = \frac{e^{-J}}{Z_t} \partial_t p_t + p_t \partial_t \left(\frac{e^{-J}}{Z_t} \right) \\ &= \frac{e^{-J}}{Z_t} \partial_t p_t - \underbrace{(\partial_t \log Z_t)}_{=p'_t} \frac{e^{-J}}{Z_t} p_t \quad (J \text{ independent of } t) \\ &= \frac{e^{-J}}{Z_t} \partial_t p_t - (\partial_t \log Z_t) p'_t. \end{aligned} \quad (6)$$

Substituting the continuity equation equation 4 into equation 6 yields

$$\partial_t p'_t = -\frac{e^{-J}}{Z_t} \nabla \cdot (p_t \mathbf{u}_t) - (\partial_t \log Z_t) p'_t. \quad (7)$$

On the other hand, for the transport term,

$$\begin{aligned} \nabla \cdot (p'_t \mathbf{u}_t) &= \nabla \cdot \left(\frac{e^{-J}}{Z_t} p_t \mathbf{u}_t \right) = \frac{e^{-J}}{Z_t} \nabla \cdot (p_t \mathbf{u}_t) + (p_t \mathbf{u}_t) \cdot \nabla \left(\frac{e^{-J}}{Z_t} \right) \\ &= \frac{e^{-J}}{Z_t} \nabla \cdot (p_t \mathbf{u}_t) - \frac{e^{-J}}{Z_t} p_t \mathbf{u}_t \cdot \nabla J = \frac{e^{-J}}{Z_t} \nabla \cdot (p_t \mathbf{u}_t) - p'_t \mathbf{u}_t \cdot \nabla J. \end{aligned} \quad (8)$$

Adding equation 7 and equation 8 gives

$$\partial_t p'_t + \nabla \cdot (p'_t \mathbf{u}_t) = -p'_t \mathbf{u}_t \cdot \nabla J - (\partial_t \log Z_t) p'_t. \quad (9)$$

If we want p'_t to be generated by the controlled field $\mathbf{u}_t + \mathbf{c}_t$, i.e.

$$\partial_t p'_t + \nabla \cdot (p'_t (\mathbf{u}_t + \mathbf{c}_t)) = 0,$$

then comparing with equation 9 we obtain the *weighted divergence equation* for \mathbf{c}_t :

$$\boxed{\nabla \cdot (p'_t \mathbf{c}_t) = p'_t (\mathbf{u}_t \cdot \nabla J + \partial_t \log Z_t)}. \quad (10)$$

Integrating equation 10 over \mathbb{R}^d and using divergence theorem,

$$\int_{\mathbb{R}^d} \nabla \cdot (p'_t \mathbf{c}_t) d\mathbf{x} = 0 \iff \int_{\mathbb{R}^d} p'_t (\mathbf{u}_t \cdot \nabla J + \partial_t \log Z_t) d\mathbf{x} = 0.$$

The identity holds because

$$\begin{aligned} \partial_t \log Z_t &= \frac{1}{Z_t} \partial_t \int e^{-J} p_t d\mathbf{x} = \frac{1}{Z_t} \int e^{-J} \partial_t p_t d\mathbf{x} = -\frac{1}{Z_t} \int e^{-J} \nabla \cdot (p_t \mathbf{u}_t) d\mathbf{x} \\ &= -\frac{1}{Z_t} \int \nabla \cdot (e^{-J} p_t \mathbf{u}_t) d\mathbf{x} + \frac{1}{Z_t} \int (p_t \mathbf{u}_t) \cdot \nabla (e^{-J}) d\mathbf{x} \\ &= \frac{1}{Z_t} \int (p_t \mathbf{u}_t) \cdot (-e^{-J} \nabla J) d\mathbf{x} = -\int p'_t \mathbf{u}_t \cdot \nabla J d\mathbf{x}, \end{aligned}$$

where the divergence integral vanishes by the boundary assumption. Hence the right-hand side of equation 10 has zero integral and equation 10 admits solutions \mathbf{c}_t (e.g. $\mathbf{c}_t = \nabla \psi_t$ with a weighted Neumann problem for ψ_t).

Step 2: Constructing a Lyapunov-compatible control. We claim that a solution \mathbf{c}_t to equation 10 can be chosen so that J relates to a local Lyapunov function as $V = -J$ under the controlled flow $\mathbf{u}_t + \mathbf{c}_t$. Decompose

$$\mathbf{c}_t(\mathbf{x}) = \mathbf{c}_t^\perp(\mathbf{x}) + \mathbf{c}_t^\top(\mathbf{x}), \quad \mathbf{c}_t^\perp(\mathbf{x}) = \alpha_t(\mathbf{x}) \frac{\nabla V(\mathbf{x})}{\|\nabla V(\mathbf{x})\|}, \quad \nabla V(\mathbf{x}) \cdot \mathbf{c}_t^\top(\mathbf{x}) \equiv 0,$$

with the convention $\alpha_t(\mathbf{x}) = 0$ at critical points $\{\mathbf{x} : \nabla V(\mathbf{x}) = 0\}$. Choose

$$\alpha_t(\mathbf{x}) = -\frac{\mathbf{u}_t(\mathbf{x}) \cdot \nabla V(\mathbf{x})}{\|\nabla V(\mathbf{x})\|} - \delta_t(\mathbf{x}) \frac{V}{\|\nabla V(\mathbf{x})\|}, \quad \delta_t(\mathbf{x}) \geq 0.$$

Then along any trajectory \mathbf{x}_t driven by $\mathbf{u}_t + \mathbf{c}_t$,

$$\frac{d}{dt} V(\mathbf{x}_t) = \nabla V(\mathbf{x}_t) \cdot (\mathbf{u}_t(\mathbf{x}_t) + \mathbf{c}_t(\mathbf{x}_t)) = -\gamma_t(\mathbf{x}_t) V(\mathbf{x}_t),$$

so V is locally Lyapunov. The tangential component \mathbf{c}_t^\top is then chosen to satisfy the residual of equation 10:

$$\nabla \cdot (p_t' \mathbf{c}_t^\top) = p_t' (\mathbf{u}_t \cdot \nabla J + \partial_t \log Z_t) - \nabla \cdot (p_t' \mathbf{c}_t^\perp),$$

which admits solutions \mathbf{c}_t^\top because both sides have zero integral.

Step 3: From Lyapunov control to guided path. Conversely, suppose there exists a control \mathbf{c}_t with

$$V = -J, \nabla V(\mathbf{x}) \cdot (\mathbf{u}_t(\mathbf{x}) + \mathbf{c}_t(\mathbf{x})) \leq -\delta V.$$

Define

$$\phi_t(\mathbf{x}) := \partial_t \log Z_t + \mathbf{u}_t(\mathbf{x}) \cdot \nabla J(\mathbf{x}),$$

and let $\tilde{\mathbf{c}}_t$ be any solution of

$$\nabla \cdot (p_t' \tilde{\mathbf{c}}_t) = p_t' \phi_t.$$

By Step 1, the controlled field $\mathbf{u}_t + \tilde{\mathbf{c}}_t$ generates p_t' . The family of solutions to the weighted divergence equation is affine; hence we can deform \mathbf{c}_t to $\tilde{\mathbf{c}}_t$ by adding a field in the nullspace of the weighted divergence operator. Choosing this adjustment tangential to the level sets of J or V (i.e. orthogonal to ∇J or ∇V) preserves the Lyapunov inequality while matching the required divergence. Thus both the Lyapunov condition and equation 10 can be enforced simultaneously.

The above derivations can easily be applied to the case $V = -kJ$ with $k > 0$.

Combing the above three steps, we complete the proof. \blacksquare

A.2.2 PROOF AND ANALYSIS OF PROPOSITION 3.3

Proposition A.2 *The following commonly used guidance strategies in generative modeling can all be interpreted as Lyapunov control within our unified framework:*

- **Classifier Guidance:** Given a trained classifier $p(\mathbf{y}|\mathbf{x})$, the Lyapunov function for guided distribution $p(\mathbf{x}|\mathbf{y})$ specified on conditioner \mathbf{y} is $V_{\mathbf{y}}(\mathbf{x}) = \log p(\mathbf{y}|\mathbf{x})$.
- **Reward Guidance:** In reinforcement learning tasks with reward function $R(\mathbf{x})$, the Lyapunov function for guided distribution $\frac{1}{Z} p_t(\mathbf{x}) e^{R(\mathbf{x})}$ concentrates probability mass in high-reward regions is $V(\mathbf{x}) = -R(\mathbf{x})$.
- **Energy-Based Model (EBM) Guidance:** For a target EBM $p(\mathbf{x}) \propto e^{-E(\mathbf{x})}$, the Lyapunov function is naturally $V(\mathbf{x}) = -E(\mathbf{x})$.
- **Image inverse problems.** Let the forward operator be $\mathbf{y} = H(\mathbf{x}) + \varepsilon$ with $\varepsilon \sim \mathcal{N}(0, \sigma^2 I)$. Then $p(\mathbf{y}|\mathbf{x}) \propto \exp(-\frac{1}{2\sigma^2} \|H(\mathbf{x}) - \mathbf{y}\|_2^2)$ and a natural Lyapunov function is $V_{\mathbf{y}}(\mathbf{x}) = \frac{1}{2\sigma^2} \|H(\mathbf{x}) - \mathbf{y}\|_2^2$, yielding guided sampling $p_t'(\mathbf{x}) \propto p_t(\mathbf{x}) \exp(-V_{\mathbf{y}}(\mathbf{x}))$ that enforces data consistency Song et al. (2023).

Proof.

- **Classifier Guidance and image inverse problems.:** Taking $J(x) = -\log p(y|x)$, we compute

$$\frac{1}{Z} p_t(x) e^{-J(x)} = \frac{p_t(x) p(y|x)}{\int p_t(x) p(y|x) dx} = \frac{p_t(x) \frac{p(x,y)}{p(x)}}{\int p_t(x) \frac{p(x,y)}{p(x)} dx} = p(x|y).$$

Thus the guided distribution is exactly conditional sampling.

- **Reward Guidance:** With $J(x) = -R(x)$, the guided law is

$$p'_t(x) = \frac{1}{Z} p_t(x) e^{R(x)},$$

which emphasizes regions of higher reward. This is equivalent to Lyapunov control with $V(x) = -R(x)$, where the control term reduces $V(x)$ along the trajectory, steering toward reward-maximizing states.

- **EBM Guidance:** If the target distribution is $p(x) \propto e^{-E(x)}$, then

$$p'_t(x) = \frac{1}{Z} p_t(x) e^{-E(x)},$$

which matches the EBM density. Interpreting $V(x) = E(x)$ as Lyapunov function, the control enforces descent in $V(x)$, aligning the flow with low-energy modes.

■

A.2.3 PROOF OF THEOREM 4.1

Theorem A.3 (Lyapunov Guarantee for Guidance) *For a candidate controller \mathbf{c} and the guidance controller space $\mathcal{U}(V) = \{\mathbf{u} : \nabla V \cdot (\mathbf{u}_t + \mathbf{c}_t) + \delta V \leq 0\}$ that rigorously satisfies the local Lyapunov condition in Proposition 3.1, define the projection operator as*

$$\pi(\mathbf{c}_t, \mathcal{U}(V)) \triangleq \mathbf{c}_t - \frac{\max(0, \nabla V(\mathbf{x}) \cdot (\mathbf{u}_t(\mathbf{x}) + \mathbf{c}_t(\mathbf{x})) + \delta V(\mathbf{x}))}{\|\nabla V(\mathbf{x})\|^2} \nabla V(\mathbf{x}).$$

Then $\pi(\mathbf{c}_t, \mathcal{U}(V))$ is locally Lipschitz continuous and thus the guided flow under $\pi(\mathbf{c}_t, \mathcal{U}(V))$ is well defined, and $\pi(\mathbf{c}_t, \mathcal{U}(V)) \in \mathcal{U}(V)$.

Proof. The local Lipschitz continuity of the projected function naturally comes from the local Lipschitz continuity of the considered functions \mathbf{u} , \mathbf{c} and V . We directly check the inequality constraint in $\mathcal{U}(V)$ is satisfied by the projection element, that is

$$\mathcal{L}_{\mathbf{u}+\mathbf{c}^*} V|_{\mathbf{c}^*=\pi(\mathbf{c}, \mathcal{U}(V))} \leq \delta - V.$$

Since the controller has affine actuator, from the definition of the Lie derivative operator, we have

$$\begin{aligned} \mathcal{L}_{\mathbf{u}+\mathbf{c}^*} V|_{\mathbf{c}^*=\pi(\mathbf{c}, \mathcal{U}(V))} &= \nabla V \cdot (\mathbf{u} + \mathbf{c} - \frac{\max(0, \mathcal{L}_{\mathbf{u}+\mathbf{c}} V + \delta V)}{\|\nabla V\|^2} \cdot \nabla V) \\ &= \nabla V \cdot (\mathbf{u} + \mathbf{c}) - \nabla V \cdot \frac{\max(0, \mathcal{L}_{\mathbf{u}+\mathbf{c}} V + \delta V)}{\|\nabla V\|^2} \cdot \nabla V \\ &= \mathcal{L}_{\mathbf{u}+\mathbf{c}} V - \max(0, \mathcal{L}_{\mathbf{u}+\mathbf{c}} V + \delta V) \leq -\delta V. \end{aligned}$$

■

A.3 RELATED WORK

Meta-learning and Task-specific Adaptation Modules. Meta-learning aims to enable models to generalize rapidly to new tasks with limited data or fine-tuning. Among various approaches, a subset of methods avoids modifying the entire network and instead introduces lightweight task-adaptive modules that guide inference without retraining the base model. Representative examples include feature-wise transformations such as FiLM layers, task-conditioning adapters, and modular meta-learning architectures (Finn et al., 2017; Rusu et al., 2019; Rebuffi et al., 2017). These methods typically operate within a meta-training/meta-testing paradigm over a distribution of tasks. In contrast, our method focuses on post-training adaptation of generative flows for new conditioning objectives, by introducing Lyapunov-inspired correction terms without retraining or task-specific fine-tuning. While sharing the spirit of lightweight adaptation, our approach is grounded in control-theoretic stability principles and ensures rigorous guarantees through a projection scheme, offering a theoretically justified alternative to heuristic task adapters.

Guidance in Generative Models. In diffusion models, classifier guidance (Dhariwal & Nichol, 2021) and classifier-free guidance (Ho & Salimans) are two influential approaches; further extensions include guidance from reward/EBM priors (Janner et al., 2022; Zhang & Xu, 2023; LeCun et al., 2006). For flow matching, recent work studies guidance at the field level and shows how importance reweighting on the joint induces pathwise changes to the marginals (Feng et al., 2025). In parallel, Sprague et al. (Sprague et al., 2024) proposed incorporating stochastic stability into flow matching, which is highly relevant to our Lyapunov control formulation. Compared with their stability-oriented modifications, our framework provides a unified *control-theoretic* view that connects diverse guidance strategies and introduces a pseudo projection operator to rigorously enforce Lyapunov inequalities at inference. Furthermore, Albergo et al. (Albergo et al., 2023) and Chen et al. (Chen et al., 2023) proposed alternative generative formulations via stochastic interpolants and phase-space bridges, respectively. While sharing a control-inspired spirit, these approaches differ fundamentally from ours: they reformulate the generative process itself, whereas we provide a general-purpose guidance scheme applicable to pre-trained flows.

Learning Certificates. Score-based modeling interprets $\nabla \log p(\mathbf{x}) = -\nabla V(\mathbf{x})$ as a learnable vector field (Song & Ermon, 2019; Song et al., 2021), while EBMs directly parametrize an energy (LeCun et al., 2006; Du & Mordatch, 2019). Few-shot or preference-based specification of priors has been explored for RL and diffusion guidance (Janner et al., 2022; Lee et al., 2025), but typically without Lyapunov certificates. Liu et al. (Liu et al., 2023a) studied physics-informed neural networks for learning and verifying Lyapunov functions in PDE systems, and Kang et al. (Kang et al., 2021) developed stable neural ODEs with Lyapunov-stable equilibria. Both are conceptually close to our Scenario 2, where we *learn* a Lyapunov candidate V_θ from sparse supervision and *jointly* enforce Lyapunov inequalities during training. Our method complements these works by focusing specifically on generative modeling and introducing an efficient projection-based stabilization scheme.

Generative Modeling in Latent or Alternative Spaces. Other approaches focus on modifying the generative space. Dockhorn et al. (Dockhorn et al., 2022) proposed score-based generative modeling in latent spaces, which reduces computational cost and enables better representation learning. Such latent guidance methods are complementary to our work: while they change the domain of generative dynamics, our framework provides a universal stabilizing principle applicable regardless of the space in which flows are defined.

A.4 NOTES ON ROBUSTNESS OF THE INITIAL VALUE

In this section, we discuss the influence of the initial value to the guided generative modelling. We note that in the original flow model, the initial data is sampled from the initial distribution p_0 . For the guided flow, we still sample the initial value from p_0 , which is common in flow matching community Lipman et al. (2023); Tong et al. (2023); Feng et al. (2025). However, according to the continuity equation, to generate p'_t in Theorem 3.2, the initial distribution should be $p'_0 = 1/Z_0 e^{-J(\mathbf{x})} p_0$ instead of p_0 . So we investigate how the choice of initial distribution influence the generation effect from the perspective of distribution convergence.

Theorem A.4 (Robustness to Initial Distribution) *Let $u_t(x)$ be the learned vector field and $c_t(x)$ the guidance control derived from Lyapunov function $V(x)$. Assume the guided field $f_t(x) = u_t(x) + c_t(x)$ satisfies the local Lyapunov condition with rate $\delta > 0$. Then, for any two initial distributions p_0 and p_0^* , the corresponding marginals p_t and p_t^* along the flow satisfy*

$$W_2(p_t, p_t^*) \leq e^{-\delta t} W_2(p_0, p_0^*), \quad \forall t \in [0, 1].$$

In particular, even if the actual inference starts from a different initial law p_0 (e.g. Gaussian noise) instead of the theoretical p_0^ , the terminal distribution at $t = 1$ remains exponentially close to the desired guided distribution $p_1^* \propto q(x)e^{-J(x)}$.*

Lemma A.5 (Lyapunov-guided field implies contraction) *Let $f_t(x) = u_t(x) + c_t(x)$ with a Lyapunov-based guidance $c_t(x) = -K_t(x)\nabla V(x)$, where $V \in \mathcal{C}^2$ and $K_t(x) \in \mathbb{R}^{d \times d}$ is symmetric positive definite. Fix a forward-invariant sublevel set $\mathcal{S}_\rho := \{x : V(x) \leq \rho\}$. Assume on \mathcal{S}_ρ :*

1. **Strong convexity of V :** $\nabla^2 V(x) \succeq mI$ for some $m > 0$;
2. **Uniform gain:** $K_t(x) \succeq \kappa I$ for some $\kappa > 0$;
3. **Bounded symmetric Jacobian of u_t :** $\frac{1}{2}(\nabla u_t(x) + \nabla u_t(x)^\top) \preceq LI$ for some $L \in \mathbb{R}$;
4. **(Optional) Slowly-varying gain:** $\|\nabla K_t(x)\| \leq B$ (if K_t depends on x).

Then, for all $x, y \in \mathcal{S}_\rho$ and $t \in [0, 1]$,

$$\langle x - y, f_t(x) - f_t(y) \rangle \leq -\delta \|x - y\|^2,$$

with

$$\delta = \kappa m - L - \varepsilon, \quad \varepsilon := \begin{cases} 0, & \text{if } K_t \text{ is constant in } x; \\ B \sup_{z \in \mathcal{S}_\rho} \|\nabla V(z)\|, & \text{otherwise.} \end{cases}$$

In particular, if $\kappa m > L + \varepsilon$, the contraction condition equation 11 holds on \mathcal{S}_ρ .

Proof. By the mean-value integral along the segment $\gamma(\theta) = y + \theta(x - y)$,

$$f_t(x) - f_t(y) = \left(\int_0^1 \nabla f_t(\gamma(\theta)) d\theta \right) (x - y).$$

Hence

$$\langle x - y, f_t(x) - f_t(y) \rangle = \int_0^1 \langle x - y, \text{sym} \nabla f_t(\gamma(\theta)) (x - y) \rangle d\theta,$$

where $\text{sym} A = \frac{1}{2}(A + A^\top)$. It suffices to upper bound $\text{sym} \nabla f_t$. Compute

$$\nabla f_t = \nabla u_t - \nabla(K_t \nabla V) = \nabla u_t - [(\nabla K_t) \nabla V^\top + K_t \nabla^2 V].$$

Taking symmetric parts yields

$$\text{sym} \nabla f_t \preceq LI - K_t \nabla^2 V + \text{sym}((\nabla K_t) \nabla V^\top).$$

On \mathcal{S}_ρ , by (A1)–(A3): $K_t \nabla^2 V \succeq \kappa m I$ and $\text{sym}((\nabla K_t) \nabla V^\top)$ has operator norm $\leq \|\nabla K_t\| \|\nabla V\| \leq B \sup_{\mathcal{S}_\rho} \|\nabla V\|$. Therefore

$$\text{sym} \nabla f_t \preceq (L - \kappa m + \varepsilon)I.$$

Integrating along $\gamma(\theta)$ gives $\langle x - y, f_t(x) - f_t(y) \rangle \leq -(\kappa m - L - \varepsilon) \|x - y\|^2$, which proves the claim with $\delta = \kappa m - L - \varepsilon$. \blacksquare

Theorem A.6 (Robustness to the Initial Distribution) Assume $c_t = -K_t \nabla V$ and conditions (A1)–(A4) in Lemma A.5 hold on a forward-invariant sublevel set; then equation 11 follows with $\delta = \kappa m - L - \varepsilon$.

Let u_t be the learned vector field and c_t the guidance control derived from a Lyapunov function V , and denote the guided field by $f_t := u_t + c_t$. Assume there exists $\delta > 0$ and a domain $\mathcal{D} \subset \mathbb{R}^d$ that is forward invariant under f_t such that

$$\langle x - y, f_t(x) - f_t(y) \rangle \leq -\delta \|x - y\|^2, \quad \forall x, y \in \mathcal{D}, \forall t \in [0, 1]. \quad (11)$$

Let p_t and p_t^* be the marginals obtained by pushing forward p_0 and p_0^* along the flow of f_t , respectively. Then, for all $t \in [0, 1]$,

$$W_2(p_t, p_t^*) \leq e^{-\delta t} W_2(p_0, p_0^*).$$

In particular, taking p_0^* as the “theoretical” initialization (e.g. the marginal induced by the conditional path), any inference initialized from a different prior p_0 (e.g. a Gaussian) remains exponentially close to the target guided law at $t = 1$.

Proof. Let $\Phi_{t,0} : \mathcal{D} \rightarrow \mathcal{D}$ denote the flow map associated with the ODE $\dot{x} = f_t(x)$, i.e., $x_t = \Phi_{t,0}(x_0)$. Fix any two initial states $x_0, y_0 \in \mathcal{D}$ and consider the distance $D(t) := \frac{1}{2} \|x_t - y_t\|^2$ where $x_t = \Phi_{t,0}(x_0)$ and $y_t = \Phi_{t,0}(y_0)$. Then

$$\dot{D}(t) = \langle x_t - y_t, f_t(x_t) - f_t(y_t) \rangle \leq -\delta \|x_t - y_t\|^2 = -2\delta D(t),$$

972 where we used equation 11. By Grönwall’s inequality,

$$973 \quad \|x_t - y_t\| \leq e^{-\delta t} \|x_0 - y_0\|, \quad \forall t \in [0, 1].$$

975 Now let γ_0 be any coupling in $\Pi(p_0, p_0^*)$. Push it forward through the product flow to obtain a
 976 coupling $\gamma_t := (\Phi_{t,0} \times \Phi_{t,0})\# \gamma_0 \in \Pi(p_t, p_t^*)$. Then

$$977 \quad \int \|x - y\|^2 d\gamma_t(x, y) = \int \|\Phi_{t,0}(x_0) - \Phi_{t,0}(y_0)\|^2 d\gamma_0(x_0, y_0) \leq e^{-2\delta t} \int \|x_0 - y_0\|^2 d\gamma_0(x_0, y_0).$$

980 Taking the infimum over all initial couplings $\gamma_0 \in \Pi(p_0, p_0^*)$ yields

$$981 \quad W_2^2(p_t, p_t^*) \leq e^{-2\delta t} W_2^2(p_0, p_0^*),$$

982 and the stated bound follows by taking square roots. ■

985 **Remark A.7 (Link to Lyapunov condition)** *The contractivity assumption equation 11 is implied*
 986 *locally if the Lyapunov control is taken as $c_t(x) = -K_t(x)\nabla V(x)$ with $K_t(x) \succeq \kappa I$, and V is m -*
 987 *strongly convex on a forward-invariant sublevel set (so that $\nabla^2 V \succeq mI$ there), while the symmetric*
 988 *part of ∇u_t is bounded above by $L_t I$ with $\kappa m - L_t \geq \delta > 0$. Then $\frac{1}{2}(\nabla f_t + \nabla f_t^\top) \preceq -\delta I$, which*
 989 *is equivalent to equation 11.*

990 This result formalizes the robustness of guided flow matching with respect to the choice of the initial
 991 distribution. Although the theoretical formulation involves the marginal initialization $p_0^* = \int p_0(x |$
 992 $x_1)q(x_1), dx_1$, in practice one typically samples directly from a Gaussian prior p_0 . The contraction
 993 guaranteed by the Lyapunov condition ensures that the discrepancy between p_0 and p_0^* vanishes
 994 exponentially fast along the trajectory. Consequently, by the terminal time $t = 1$, the generated
 995 distribution p_1 is already arbitrarily close to the target law, making inference from p_0 both valid and
 996 effective.

998 A.5 EXPERIMENTAL CONFIGURATIONS AND ADDITIONAL EXPERIMENTS

1000 A.5.1 SYNTHETIC DATA EXPERIMENTS.

1001 For the 2D synthetic benchmarks (uniform-to-8Gaussians, circle-to-S-curve and 8Gaussians-to-
 1002 Moons), we follow the setup of (Feng et al., 2025). The flow model is trained with displacement
 1003 interpolation and a 4-layer MLP with hidden dimension 128, using Adam optimizer with learning
 1004 rate 10^{-4} . Each experiment is trained for 20k iterations with batch size 512. Guidance baselines
 1005 include Monte Carlo (g^{MC}), covariance-based guidance ($g^{\text{cov-A}}$, $g^{\text{cov-G}}$), contrastive energy guid-
 1006 ance (CEG), and learned guidance g_ϕ . For each method, we apply our pseudo projection operation
 1007 (LyaGuide-ES/AS/CS) in the inference stage.

1008 **Few-shot Supervision (Scenario 2).** In Scenario 2, we subsample preference data–score pairs with
 1009 sizes varying from 128 to 1024. The Lyapunov candidate V_θ is parameterized as an MLP with 3
 1010 hidden layers (width 64) and trained using weighted regression. We emphasize low-score samples
 1011 to encourage convexity around minima. Once V_θ is learned, the corresponding guidance control is
 1012 synthesized using either explicit descent or integrated into g_ϕ .

1026
 1027
 1028
 1029
 1030
 1031
 1032
 1033
 1034
 1035
 1036
 1037
 1038
 1039
 1040
 1041
 1042
 1043
 1044
 1045
 1046
 1047
 1048
 1049
 1050
 1051
 1052
 1053
 1054
 1055
 1056
 1057
 1058
 1059
 1060
 1061
 1062
 1063
 1064
 1065
 1066
 1067
 1068
 1069
 1070
 1071
 1072
 1073
 1074
 1075
 1076
 1077
 1078
 1079

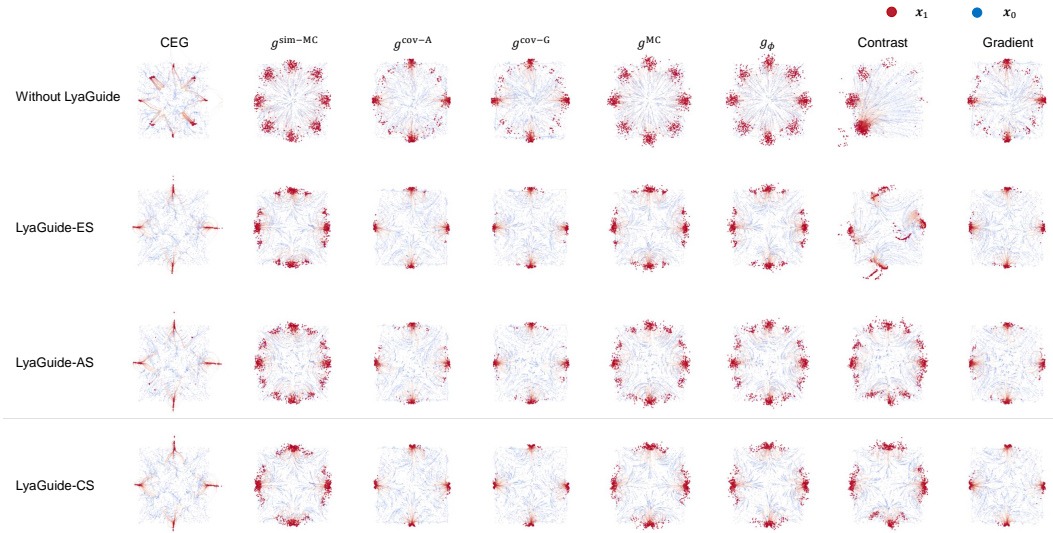


Figure 5: Scenario 1 results in 8-Gaussian task with different variants of LyaGuide.

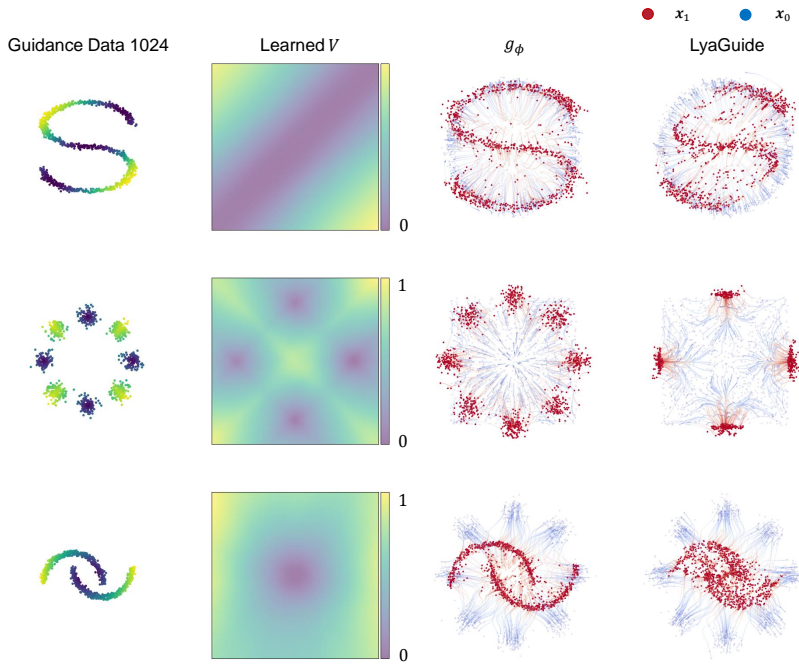


Figure 6: Scenario 2 results on synthetic data with dataset size = 1024.

1080
 1081
 1082
 1083
 1084
 1085
 1086
 1087
 1088
 1089
 1090
 1091
 1092
 1093
 1094
 1095
 1096
 1097
 1098
 1099
 1100
 1101
 1102
 1103
 1104
 1105
 1106
 1107
 1108
 1109
 1110
 1111
 1112
 1113
 1114
 1115
 1116
 1117
 1118
 1119
 1120
 1121
 1122
 1123
 1124
 1125
 1126
 1127
 1128
 1129
 1130
 1131
 1132
 1133

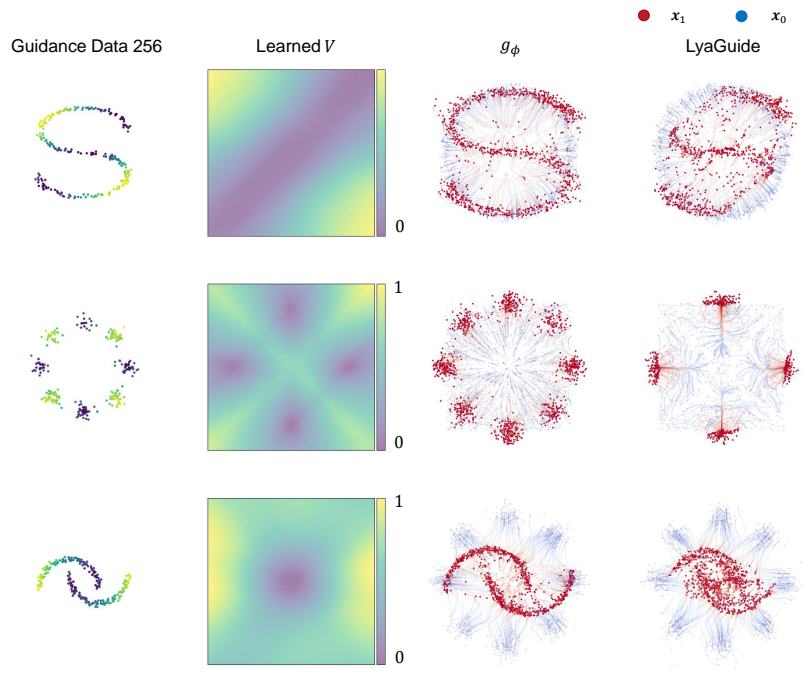


Figure 7: Scenario 2 results on synthetic data with dataset size = 256.

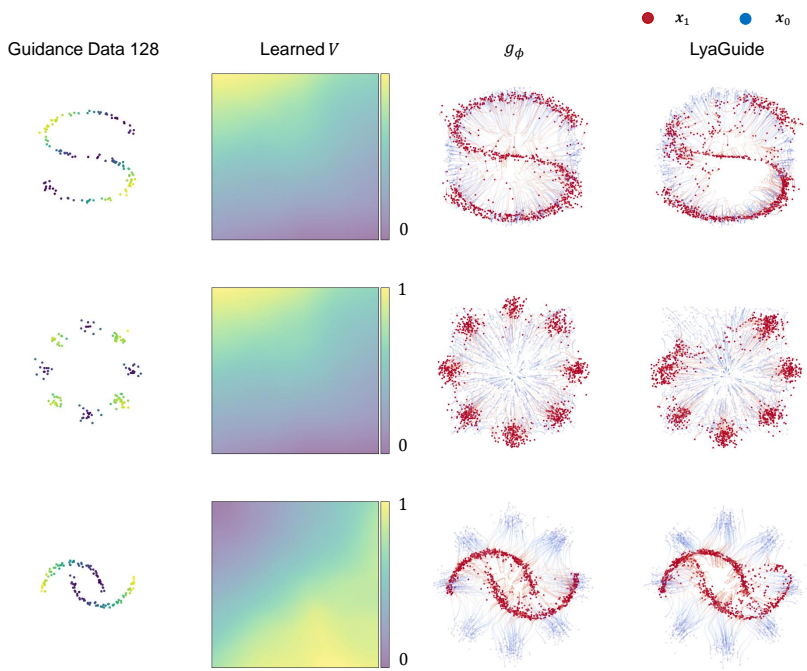


Figure 8: Scenario 2 results on synthetic data with dataset size = 128.

A.5.2 IMAGE INVERSE PROBLEMS.

For CelebA-HQ image inpainting, deblurring, and super-resolution tasks, we adopt the same experimental protocol as (Song et al., 2023; Feng et al., 2025). Conditional flow matching (CFM) and optimal-transport CFM (OT-CFM) are used as base models. Evaluation metrics include FID, LPIPS, PSNR, and SSIM over 3000 test samples. Baselines (g^{MC} , g^{cov-A} , IIGDM, etc.) are compared with and without LyaGuide projection. Hyperparameters for the pseudo projection are fixed across all tasks, demonstrating robustness without extra tuning.

Table 2: Image inverse problem results on CelebA-HQ (Super-Resolution task).

		Original Methods				LyaGuide-ES				LyaGuide-CS			
		FID ↓	LPIPS ↓	PSNR ↑	SSIM ↑	FID ↓	LPIPS ↓	PSNR ↑	SSIM ↑	FID ↓	LPIPS ↓	PSNR ↑	SSIM ↑
OT-CFM	g^{cov-A}	30.2284	0.3713	22.9642	0.5988	30.2183	0.3712	22.9707	0.5992	27.5309	0.3630	22.8065	0.6132
	g^{sim-A}	31.8224	0.3718	23.8667	0.6069	31.5397	0.3705	23.8698	0.6091	27.5309	0.3630	22.8065	0.6132
	IIGDM	22.9596	0.2826	26.9492	0.7584	23.0441	0.2827	26.9462	0.7582	23.7278	0.2854	26.9099	0.7554
	g^{MC}	24.1797	0.5521	8.7411	0.3628	24.9576	0.5538	8.8167	0.3637	25.3356	0.5430	9.0702	0.3848
CFM	g^{cov-A}	31.9606	0.3769	22.7715	0.5897	32.0031	0.3769	22.7778	0.5902	31.2359	0.3741	22.7429	0.5948
	g^{sim-A}	32.6209	0.3745	23.6848	0.6005	31.9223	0.3712	23.6621	0.6061	27.7175	0.3564	23.4357	0.6312
	IIGDM	25.7605	0.2900	26.8810	0.7470	25.9728	0.2897	26.8811	0.7473	26.7152	0.2933	26.8322	0.7434
	g^{MC}	26.5714	0.5555	8.9762	0.3588	28.1408	0.5566	9.0434	0.3595	27.7506	0.5456	9.3742	0.3836

Table 3: Image inverse problem results on CelebA-HQ (Gaussian deblurring task).

		Original Methods				LyaGuide-ES				LyaGuide-CS			
		FID ↓	LPIPS ↓	PSNR ↑	SSIM ↑	FID ↓	LPIPS ↓	PSNR ↑	SSIM ↑	FID ↓	LPIPS ↓	PSNR ↑	SSIM ↑
OT-CFM	g^{cov-A}	15.7897	0.2738	26.0362	0.7202	14.9309	0.2699	26.2131	0.7247	11.9049	0.2534	26.2578	0.7375
	g^{sim-A}	14.7355	0.2506	27.8596	0.7721	14.9201	0.2507	27.8551	0.7720	14.7920	0.2500	27.8420	0.7719
	IIGDM	20.4083	0.2514	28.6943	0.7827	19.8694	0.2492	28.7049	0.7838	20.3166	0.2517	28.6720	0.7820
	g^{MC}	24.5336	0.5524	8.7690	0.3640	28.0601	0.5156	10.5469	0.4110	27.5108	0.5388	9.2243	0.3913
CFM	g^{cov-A}	16.6399	0.2830	25.5352	0.6989	16.0158	0.2792	25.6866	0.7031	13.1084	0.2641	25.7225	0.7161
	g^{sim-A}	15.2263	0.2591	27.5387	0.7587	15.2263	0.2591	27.5387	0.7587	15.6122	0.2585	27.4902	0.7581
	IIGDM	20.7786	0.2593	28.3883	0.7709	20.3063	0.2557	28.5493	0.7750	20.6238	0.2591	28.4349	0.7709
	g^{MC}	26.4901	0.5556	9.0386	0.3612	31.1472	0.5276	10.3195	0.3959	30.0128	0.5410	9.5963	0.3917

1188
 1189
 1190
 1191
 1192
 1193
 1194
 1195
 1196
 1197
 1198
 1199
 1200
 1201
 1202
 1203
 1204
 1205
 1206
 1207
 1208
 1209
 1210
 1211
 1212
 1213
 1214
 1215
 1216
 1217
 1218
 1219
 1220
 1221
 1222
 1223
 1224
 1225
 1226
 1227
 1228
 1229
 1230
 1231
 1232
 1233
 1234
 1235
 1236
 1237
 1238
 1239
 1240
 1241



Figure 9: The visualization of the image inverse problems with the base flow matching model of mini-batch optimal transport conditional flow matching (OT-CFM). Four rows show the results of four baselines with the corresponding LyaGuide results in box-inpainting task.

1242
 1243
 1244
 1245
 1246
 1247
 1248
 1249
 1250
 1251
 1252
 1253
 1254
 1255
 1256
 1257
 1258
 1259
 1260
 1261
 1262
 1263
 1264
 1265
 1266
 1267
 1268
 1269
 1270
 1271
 1272
 1273
 1274
 1275
 1276
 1277
 1278
 1279
 1280
 1281
 1282
 1283
 1284
 1285
 1286
 1287
 1288
 1289
 1290
 1291
 1292
 1293
 1294
 1295



Figure 10: The visualization of the image inverse problems with the base flow matching model of conditional flow matching (CFM). Four rows show the results of four baselines with the corresponding LyaGuide results in box-inpainting task.